EUROPEAN ORGANIZATION FOR NUCLEAR RESEARCH
CERN — SL DIVISION

CERN-SL-98-033 (EA)

NA48 Note 98-16

THE SIMULTANEOUS LONG- AND SHORT-LIVED NEUTRAL KAON BEAMS FOR EXPERIMENT NA48

C.Biino [1], N.Doble [2], L.Gatignon [2], P.Grafström [2] and H.Wahl [3]

Abstract

Simultaneous, nearly-collinear beams of long- and short-lived neutral kaons are an essential feature of the precision CP-violation experiment NA48 *) at the SPS. The present report describes the design and performance of these beams in relation to the requirements of the experiment.

[1] SL-, now EP-Division,
[2] SL-Division,
[3] EP-Division.

*) Cagliari-Cambridge-CERN-Dubna-Edinburgh-Ferrara-Florence-Mainz-Orsay-Perugia-Pisa-Saclay-Siegen-Torino-Vienna-Warsaw Collaboration.

Geneva, Switzerland
May 1998

Introduction

A pair of simultaneous, nearly-collinear beams of long- and short-lived neutral kaons constitutes an integral part of experiment NA48 at the SPS. The design, construction, installation and control of the beam lines and their components formed the object of a project (SL-24), under responsibility of SL Division.

The experiment is designed to measure the parameter ε'/ε, which is indicative of 'direct' CP-violation in $K^0 \rightarrow 2\pi$ decay, to a precision of $2 \cdot 10^{-4}$, [1]. The principle of the measurement depends on comparing the relative decay rates into two neutral and into two charged pions of the long- and short-lived neutral kaons (K_L and K_S, respectively).

The parameter ε'/ε is related to the measured double ratio of the $K^0 \rightarrow 2\pi$ decay rates via the relation:

$$\frac{\varepsilon'}{\varepsilon} = \frac{1}{6}\left[1 - \frac{\left(K_L \rightarrow 2\pi^0 \rightarrow 4\gamma\right)/\left(K_L \rightarrow \pi^+\pi^-\right)}{\left(K_S \rightarrow 2\pi^0 \rightarrow 4\gamma\right)/\left(K_S \rightarrow \pi^+\pi^-\right)}\right]$$

The following sections are intended to constitute the Chapter on: '**The Neutral Kaon Beams**', written as part of a technical paper entitled: '**The Beam and Detector for the Precision CP-Violation Experiment NA48'**, to be published by the NA48 collaboration. An abridged version will also appear as a contribution to the 1998 European Particle Accelerator Conference in Stockholm.

1 Design concept

In order to minimise systematic differences in the relative measurement of the decay rates: $K_L \rightarrow \pi^0\pi^0$, $K_L \rightarrow \pi^+\pi^-$ and $K_S \rightarrow \pi^0\pi^0$, $K_S \rightarrow \pi^+\pi^-$, beams of long- and short-lived neutral kaons, $\mathbf{K_L}$ and $\mathbf{K_S}$, are required to enter the same fiducial region **simultaneously** and **nearly-collinearly**, converging at a small angle towards a common set of detectors, [1]. The principle is shown in Figure 1.

Whereas a primary proton beam of high energy (450 GeV) and high flux (~10^{12} protons/s) is required to produce sufficient $K_L \rightarrow 2\pi$ decays, a proton flux that is lower by a factor ~10^{-5}, (given roughly by the square of the CP-violating, $K_L \rightarrow 2\pi$ decay amplitude: $|\eta^{00}|^2 \approx |\eta^{+-}|^2$), suffices to produce a comparable number of K_S decays. The lower flux renders possible the attribution of the detected decays to K_S or K_L by **tagging** the protons used to produce the $\mathbf{K_S}$.

The protons which produce the K_S are obtained by splitting off a small fraction of the primary beam, taking advantage of the phenomenon of 'channeling' in a bent crystal. The method adopted combines the functions of reducing the flux, deflecting the selected protons away from accompanying background and defining a beam of small emittance, well-suited to produce the K_S.

The acceptances for detecting the $\pi^0\pi^0$ and $\pi^+\pi^-$ decays are each functions of the kaon momentum (p_K) and longitudinal position of the decay vertex (z). It is therefore important to render the momentum spectra of the K_L and K_S decays as similar as possible over the useful range of momenta: (70 GeV/c < p_K < 170 GeV/c) and over the range of z, which is chosen proportional to the K_S mean decay-length, $\lambda_S = \tau_S \cdot p_K/m_K \approx 5.4\ \text{m} \cdot (p_K/100\ \text{GeV/c})$. Weighting factors (which depend only on the life-times: τ_S and τ_L) can then be applied to render the z-distributions and hence the acceptances equal for K_S and K_L decays.

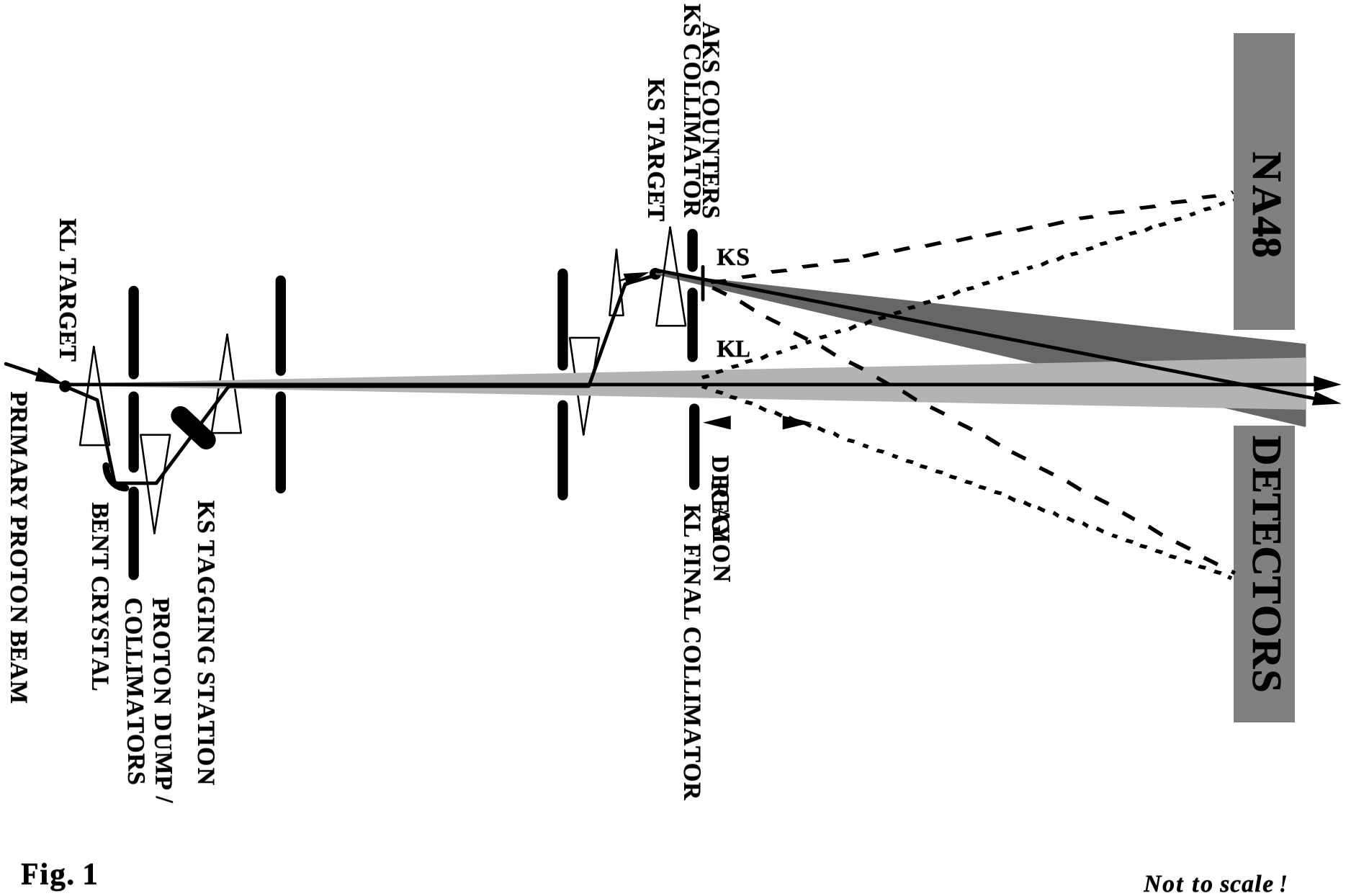

Fig. 1

Figure 1: Principle of simultaneous, nearly-collinear K_L and K_S beams.

2. The simultaneous K_L and K_S beams

2.1 Layout:

A branch of the 450 GeV/c primary proton beam, slow-extracted from the CERN Super-Proton-Synchrotron (SPS) towards the North Area, is used to produce the neutral kaon beams. These are installed in a 270 m long, underground tunnel complex, designed for high intensities, [2]. Due to the different mean decay-lengths of K_L and K_S (λ_L=3480 m, λ_S=6.0 m, respectively, for a mean p_K=110 GeV/c), the beams are derived from protons striking two separate targets, respectively situated 126 m and 6.0 m upstream of the beginning of the common decay region. The longer length of the K_L beam is chosen to ensure that the K_S component in that beam has decayed to a proportion of $\sim 5 \cdot 10^{-8}$, averaged over the useful range of p_K, or $\sim 1 \cdot 10^{-6}$ at the highest momentum considered.

The layout of the simultaneous K_L and K_S beams is shown schematically, in vertical section, in Figure 2 and the nominal design characteristics of the beams are listed in Table I.

2.2 Primary proton transport to the K_L target:

The 450 GeV/c primary proton beam, emerging from an upstream target station (T4), passes through a pair of dump/collimators to select the wanted flux of, nominally, $1.5 \cdot 10^{12}$ protons per SPS pulse (2.38 s spill every 14.4 s). This beam is transported over a distance of 838 m and is finally focused and directed vertically downwards at an angle of 2.4 mrad., onto the K_L target. The optics incorporates an intermediate focus at a point, where a steering magnet (Trim 5) is placed, which specifically allows the angle of the beam onto the target to be adjusted horizontally, (Section 2.7). Small changes in this angle do not significantly change the total angle of 2.4 mrad., at which the K_L beam is produced.

The choice of 2.4 mrad. compared to zero production angle reduces the total flux of neutrons per useful K_L by a factor ~4 (to ~10 : 1), for only ~25% reduction in the useful K_L per proton. In fact, it minimises the product of the ratios of primary protons and of secondary neutrons, each with respect to the flux of useful K_L obtained. These ratios relate to the relative backgrounds from proton- and neutron-induced sources.

2.3 The K_L target station:

The detailed layout of the K_L target station is shown schematically, in vertical section, in Figure 3. Its principal components are surrounded with iron followed by concrete shielding.

The K_L target consists of a 2 mm diameter, 400 mm long rod of beryllium, made in four sections, each suspended between thin aluminium foils. It is precisely aligned along the (horizontal) K_L beam axis and is immediately followed by a water-cooled, copper collimator of 15 mm aperture, through which the neutral (K_L) and the remaining primary proton beams exit. A 10.8 T.m, vertically-deflecting, dipole magnet (B 1 in Fig. 3) then serves to sweep away charged particles, whereby the primary protons are deflected further downwards by 7.2 mrad. At a distance of 10.95 m from the target they impinge on a bent crystal, centred 72 mm below the K_L beam axis. The crystal is designed to split off a wanted, small fraction of the protons by deflecting them through an upward angle of 9.6 mrad., back to the horizontal. The majority of the protons and other particles, not channeled by the crystal, continue undeviated. With the exception of muons, they are absorbed in the water-cooled, copper blocks of the following pair of beam-dump/collimators (TAX 17 + 18), which are fitted with tungsten-lined passages for the wanted beams. Thus the aperture for the K_L beam in TAX 18 (8 mm diameter) limits the neutral beam to ~3 times its final acceptance.

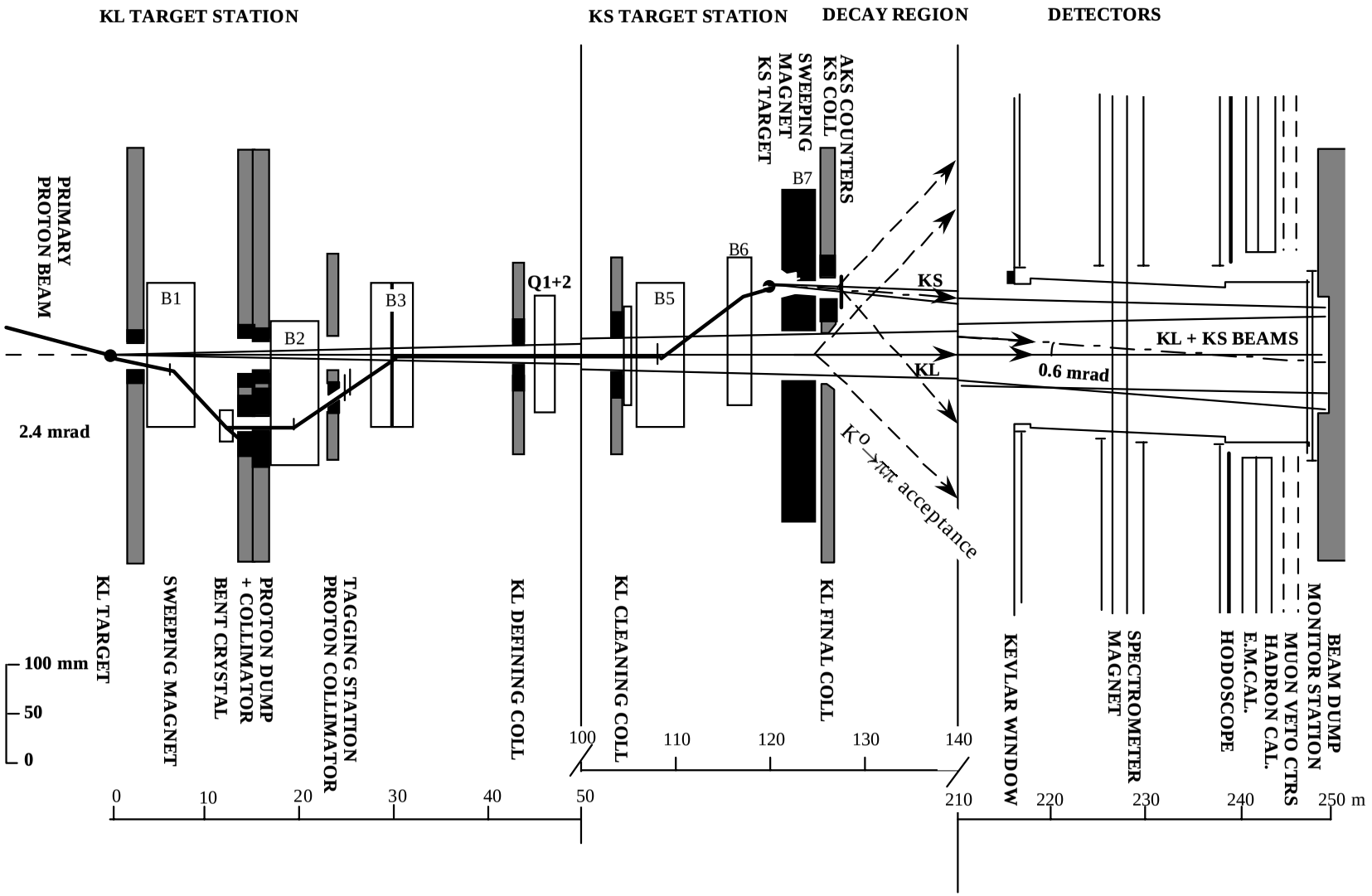

Fig. 2

Figure 2: Schematic layout of K_L + K_S beams, (vertical section).

TABLE I **Design Characteristics of the Simultaneous K_L + K_S Beams**

	K_L	K_S
Primary protons per pulse on target	$1.5 \cdot 10^{12}$	$3 \cdot 10^7$
SPS Spill length (s) / Cycle time (s)	2.38 / 14.4	
Proton momentum, p_o (GeV/c)	450	450
Production angle of K^0 beam (mrad.)	2.4	4.2
Length of K^0 beam : target to final collimator/AKS (m) target to front of e.m.calorimeter (m)	 126.00 241.10	 6.07 121.10
Angle of convergence to K_L (mrad.)	0.0	-0.6
Angular acceptance of beam (mrad.)	±0.15	±0.375
R.M.S.radius at e.m.calorimeter (mm)	~26	~39
Useful momentum range,p_K (GeV/c)	$70<p_K<170$	
Fiducial length for decays, $z=4\lambda_S$ (m)	$\sim 15<z<\sim 36$	
K^0-flux per pulse at exit final coll.	$\sim 2 \cdot 10^7$	$\sim 2 \cdot 10^2$
- decays between coll. and detector	$\sim 1.4 \cdot 10^6$	$\sim 2 \cdot 10^2$
K^0-flux per pulse in useful p_K range	$6.4 \cdot 10^6$	$1.5 \cdot 10^2$
- decays per pulse in p_K range and fiducial length	$4.4 \cdot 10^4$	$1.5 \cdot 10^2$
- decays per pulse to $\pi^0\pi^0$ in pK range and fiducial length	40	45
Detector acceptance for $\pi^0\pi^0$ decays	~0.20	
Useful $K^0 \rightarrow \pi^0\pi^0$ detected per pulse - per year (125 days with overall efficiency 0.5)	~8 $\sim 3.0 \cdot 10^6$	~9 $\sim 3.4 \cdot 10^6$

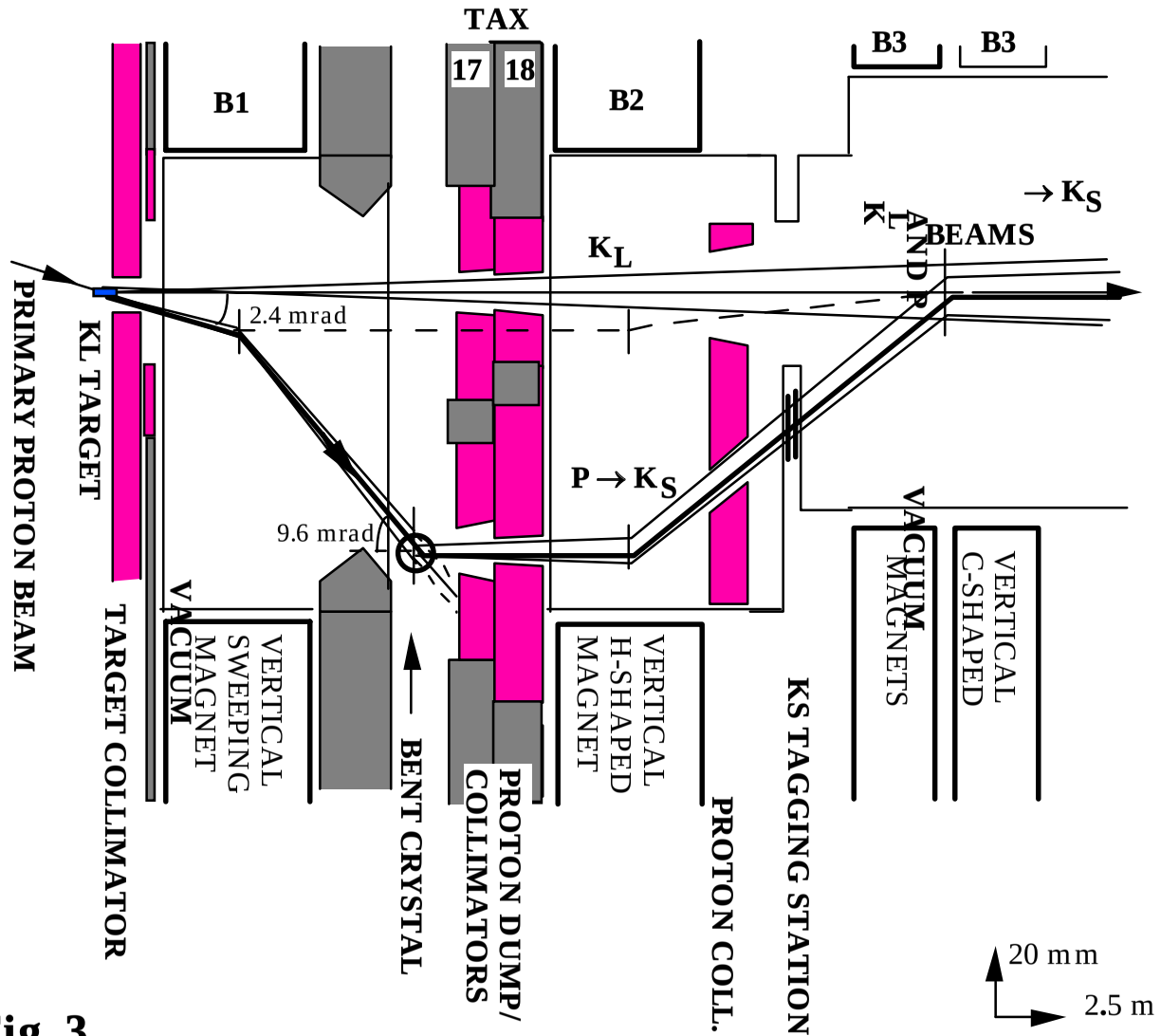

Fig. 3

Figure 3: Detailed layout of the K_L target station and of the proton beam trajectory via the bent crystal 'splitter' to the K_S - TAGGING STATION, (vertical section). (The dashed line shows the trajectory followed by the π^- + K^-calibration beam described in Section 4.2).

2.4 K_L beam collimation:

The neutral (K_L) beam is collimated in three successive stages by 'defining', 'cleaning' and 'final' collimators, shown in Figure 4.

The final collimator is set back from the beginning of the fiducial volume by a distance typically three times the z-resolution of reconstructed K_L-decay vertices, so as not to affect the counting of these decays. It is located from 120.7 to 124.3 m from the target and has an aperture (from 54 to 57.5 mm diameter), which fits in the gap of the last sweeping magnet. This is preceded by the cleaning collimator, of such aperture as to prevent particles produced or scattered on the edges of the defining collimator from striking the final collimator. It is located ~20 m, or ~$3\lambda_S$, upstream of the latter, to let K_S, which may be regenerated on its edges, decay away before reaching the fiducial volume. The condition that particles from the target should not strike the cleaning collimator directly leads to an optimum longitudinal position (~41 m) and aperture (12.2 mm diameter) for the defining collimator, that maximise the acceptance of the neutral beam.

The projection of straight lines, joining opposite sides of the apertures of the defining- and cleaning-collimators defines a 'penumbra' around the K_L beam, (shown in Fig. 4). This is not allowed to intercept any material further downstream and thus defines minimum apertures for the passage of the beam through the centre of the various detectors.

In fact, it is essential for the collimation scheme, that the neutral beam (K_L, accompanied by neutrons and photons) and also the proton beam for the K_S be transported in vacuum over practically the full length from the exit of the target through to the final beam dump downstream of the detectors. The only exception permitted occurs at the location of the crystal and dump/collimators belonging to the target station, where the vacuum is interrupted by thin windows separated by a 4.6 m long passage through air.

The defining and cleaning collimators each consist of a 1.2 m long steel block containing a cylindrical bore, fitted with a series of tungsten-alloy inserts of graduated aperture. The block is housed in a vacuum chamber, which, as a whole, is capable of small transverse displacements with respect to the adjoining beam tube. Moreover, the block can itself be raised out of or lowered into position on the beam. Thus, each collimator can in turn be brought into line with the axis of the neutral beam, as defined initially by the target and the final collimator, observing the centres of the profiles at the MONITOR STATION at the end of the beam line (see Fig. 2 and Section 3.1).

2.5 Muon background:

A high flux of muons, from the decay of charged pions (and kaons) produced in the K_L target and beam dump, would naturally reach the detectors. They present a special problem in the case of the simultaneous beams, where the positions, polarities and strengths of sweeping magnets are constrained by the need also to transport protons further downstream to produce the K_S. Within these constraints, the layout of beam elements has been designed to minimise the muon flux into the detectors with the aid of the simulation programme, 'HALO', [3].

The first magnet after the target (B 1 in Fig. 3) deflects positive particles downwards and negative particles upwards. It is vitally important that this action is not cancelled by the following, upward deflection needed to recuperate the protons. This is provided by the highly-selective, bent crystal, in place of a magnet.

Downstream of the beam dump, use is made of the same-sign fields in the top yoke and aperture of successive, vertical H- and C-shaped magnets, belonging to the proton transport (B 2 and B 3 in Fig. 3), to increase the upward deflection of μ^-. The opposite fields in their respective lower yokes have little net effect on the μ^+.

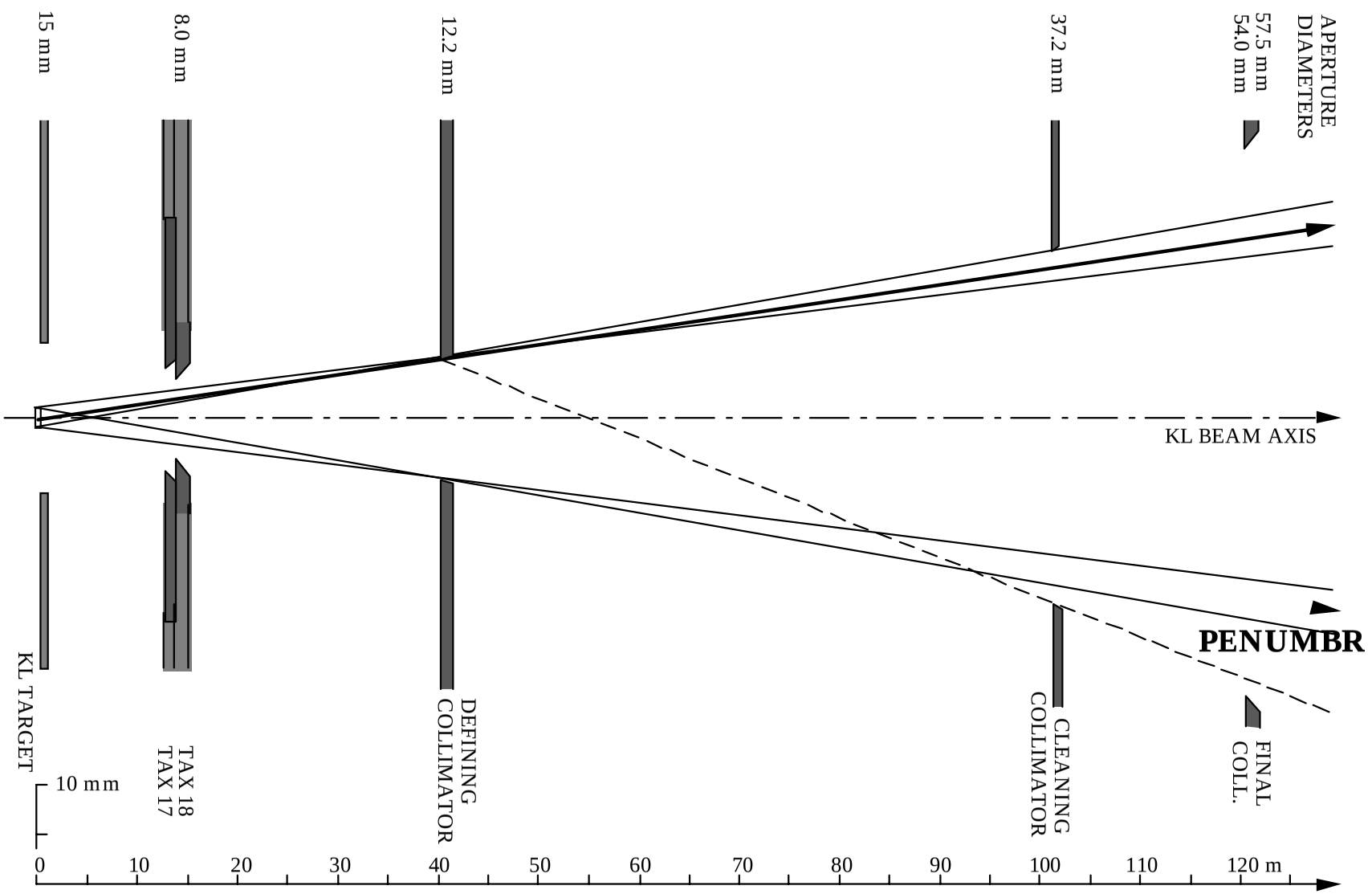

Fig. 4

Figure 4: Schematic layout of the K_L beam collimation scheme.

A 5 m long, toroidally-magnetised, iron 'scraper', surrounding the beam, is then designed to defocus any remaining μ^-, whilst focusing the μ^+ towards a series of three, 2 m long, H-shaped magnets of large cross-section. The space between their poles is filled with a slab of soft-iron, through which a 40 mm diameter hole has been bored to let the proton beam pass almost undeflected. The surrounding muons, however, encounter a mainly vertically-directed field integral of ~9 T.m and are hence deflected by an angle in the horizontal plane, which exceeds their r.m.s. multiple scattering in the iron by a factor ~10, and is sufficient to clear the downstream detectors.

At nominal primary proton flux, residual *background* muons originating from the K_L target station and traversing the area (~5 m^2) of the detectors are counted to be $1.6 \cdot 10^5$ per SPS pulse, (see Table II), an order of magnitude lower than observed with the magnetic sweeping downstream of the dump switched off (Section 4.1).

2.6 The bent crystal:

When charged particles enter a crystal within a small ('critical') angle to its planes, the collective Coulomb fields can cause them to be 'channeled'. If the crystal is mechanically bent, some of the particles still follow the planes and are thus deflected. Most experiments which have studied this effect for high-energy protons have used a parallel incident beam, in order to maximise the transmission into the deflected beam, e.g. [4]. Instead, the present application requires only a small fraction (nominally $5 \cdot 10^{-5}$) of those protons to be deflected which diverge towards the crystal from a focal point at the K_L target. The crystal holder should allow the angle of deflection to be fine-tuned, whilst being insensitive to heat and irradiation by ~10^{12} protons/cm^2 per pulse, resulting in an annual exposure to ~10^{18} protons/cm^2 [1]

The solution adopted has been described in detail, [6], and is shown schematically in Figure 5. A mono-crystal of silicon, cut to dimensions of $[60 \cdot 18 \cdot 1.5]$ mm^3, parallel to the (110) planes, is used. It is bent through an angle, $\theta_O = 18.7$ mrad. (greater than the required beam deflection angle, $\theta = 9.6$ mrad.) over 56 mm of its length, by pressing it against the cylindrical surface of an aluminium block, which has been precisely machined to the specified radius of curvature, (R=3.0 m). The crystal holder is in turn mounted on a motorised goniometer, which allows the crystal to be aligned on the incident beam with two transverse displacements and two angular rotations about axes perpendicular to the beam. When the crystal is rotated through an azimuthal angle, $\phi \approx \pm 28.7^\circ$ (about the vertical axis), the beam impinges on one side edge, traverses the crystal diagonally and exits from the opposite edge, (Fig. 5). The effective, fractional length of the bent crystal traversed, and hence the vertical angle of deflection of the beam, is then governed by adjusting the angle ϕ. Moreover, a coupling (given by: $dy'/dx = 1/R \cdot \tan\phi$) is introduced between the vertical angle (y') and the lateral position (x) of the protons that can be channeled. This has the advantage that the horizontal as well as the vertical emittance of the beam is defined by the crystal.

2.7 Proton transmission:

The experiment nominally requires a fraction of $2 \cdot 10^{-5}$ of the protons incident on the K_L target (~$5 \cdot 10^{-5}$ of those not absorbed in the target) to be deflected and transmitted to produce the K_S beam. With the parameters chosen for the crystal and the optics of the proton beam used initially, an

[1] By comparison, a silicon crystal, previously exposed to a localised, integrated fluence of $2.4 \cdot 10^{20}$ protons/cm^2 at the SPS, has shown a reduction in channeling efficiency of (31±4)% in the region of irradiation, when used in a bending experiment, [5].

TABLE II **Typical Counting Rates in NA48 Detectors**

	MEASURED Sep. 1997			**ANALYSED** and **SCALED** to **nominal proton fluxes**			
COUNTING RATES per SPS pulse :	**BEAM MODE :**			**CONTRIBUTIONS :**			**TOTAL**
	$[K_L]$	$[K_S]$	$[K_L+K_S]$	K_L	K_S	*Bkgrd.*	$\mathbf{K_L+K_S}$
Protons to K_L TARGET $* 10^{12}$	1.06	1.06	1.06	**1.5**	**-**	**1.5**	**1.5**
Protons to K_S TARGET via TAGGING STATION $* 10^7$	**-**	3.4	3.4	**-**	**3.0**	**-**	**3.0**
K_S monitor telescope (KSM) $* 10^5$	0.1	2.3	2.4	0.1	2.0	0.0	**2.1**
AKS counters - with aligned Ir-crystal converter $* 10^4$ (>2 min. ionizing particles)	0.0	5.2	5.2	0.0	4.6	0.0	**4.6**
Sum of AKL anti-counters $* 10^6$	4.4	3.6	5.0	2.0	0.6	4.2	**6.8**
Sum of WC 1 $* 10^6$	1.5	0.7	1.6	1.2	0.07	0.9	**2.2**
Sum of WC 4 $* 10^6$	1.2	0.4	1.2	1.1	0.05	0.5	**1.7**
Sum of charged hodoscope V-plane (QV-OR) $* 10^6$	1.6	0.6	1.6	1.5	0.07	0.7	**2.3**
Coincidence of hodoscope V + H-planes (QV.QH) $* 10^6$	1.0	0.3	1.1	1.1	0.05	0.4	**1.5**
Coincidence of hodoscope opposite quadrants (QX) $* 10^5$	6.7	0.6	7.0	9.0	0.3	0.4	**9.7**
QX coincidence with μ-veto (QX.MU) = $K\mu 3$ $* 10^5$	1.5	0.1	1.5	2.0	0.0	0.1	**2.1**
Neutral hodo. in e.m. cal. $* 10^5$	0.8	<~0.01	0.8	1.2	<~0.01	0.0	**1.2**
Coincidence of hadron cal. opp. quadrants (HAC-K) $* 10^5$	1.8	0.02	1.8	2.6	~0.01	0.0	**2.6**
Muons (MU.Q-OR) $* 10^5$	2.8	1.1	2.8	2.3	~0.01	1.6	**3.9**
Beam counter (BCTR H.V) - with 5 mm Al converter $* 10^6$	3.4	~0.001	3.4	5.0	~0.001	-	**5.0**

BENT CRYSTAL:

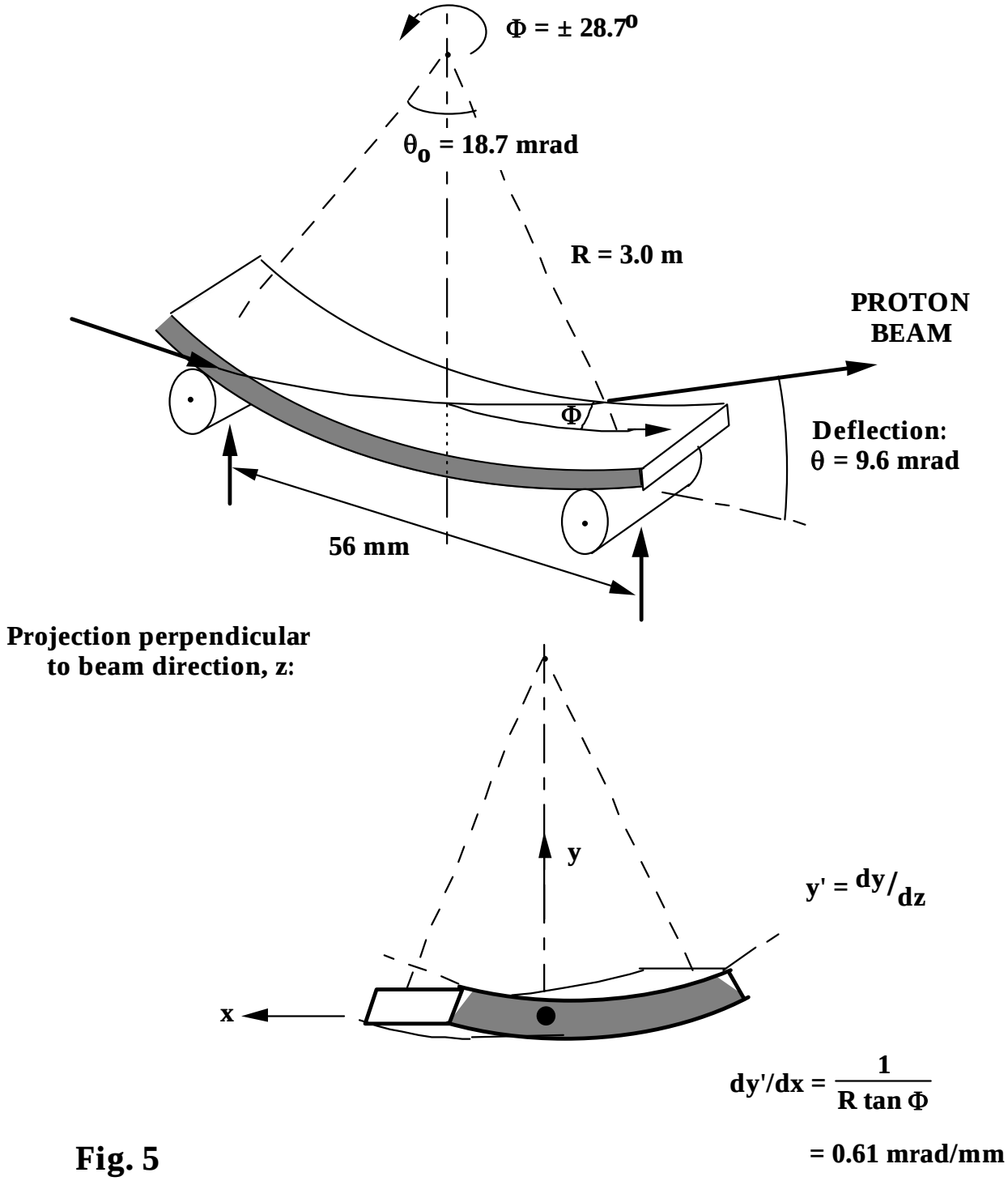

Figure 5: Schematic arrangement of the bent crystal.

overall transmission of ~$3 \cdot 10^{-5}$ is observed when the proton beam is centred on the crystal. The transmission can be reduced by increasing the horizontal extent of the beam incident on the crystal. In fact, the focusing of the proton beam was arranged to give a large (factor 3) magnification in horizontal beam divergence at the K_L target and it is possible to increase this further to obtain the nominal transmission. Another way to reduce the transmission consists of changing the horizontal angle of the whole beam about the centre of the K_L target, by means of an upstream steering magnet (Trim 5, see Section 2.2). This reduces the local intensity of protons that strike the crystal over the small horizontal extent (~±0.2 mm), in which the conditions for channeling are fulfilled. The transmission of protons monitored at the TAGGING STATION, (see Fig. 3 and Section 3.1), is plotted in Figure 6 as a function of the current in Trim 5.

It is important for the cancellation of the effect of background in the detectors that the ratio of K_S to K_L fluxes remains constant or is monitored to within ~±10% over each SPS pulse. The K_S flux is sensitive to the angle of the proton beam at the K_L target (Fig. 6) and hence to time-variations of the beam extracted from the SPS. Instantaneous rates variously related to K_S and K_L are therefore recorded by the AKS counters (shown in Figs. 2 and 8), a counter telescope (KSM) viewing the K_S target and by a counter array (BCTR) predominantly sensitive to the K_L beam at the MONITOR STATION, (see Fig. 2 and Section 3.1). The counting rates are displayed each pulse and are used when necessary to adjust the current in Trim 5 to render the K_S/K_L ratio nearly constant, as shown typically in Figure 7.

2.8 Proton transport to the K_S target:

The second of the beam dump/collimators downstream of the crystal (TAX 18) contains a set of tungsten-alloy inserts with graduated apertures of smallest diameter 2.4 mm, aligned on an axis 72 mm below and parallel to that of the K_L beam, (Fig. 3). This passage is matched to the proton beam defined by the crystal. There follows the H- and C-shaped magnets of opposite polarity (B 2 and B 3), which successively deflect the transmitted protons back towards and then onto the K_L beam axis. In between these, the protons pass through the TAGGING STATION, which is installed in a space 36 mm below the K_L axis and is preceded by a protecting collimator, fitted with separate passages for the proton and K_L beams.

On the K_L beam axis, the protons are steered through the defining and cleaning collimators and are refocused by a series of quadrupole magnets (Q 1 + 2 in Fig. 2) to a point 109 m downstream of the crystal. Before reaching this focus, they are again deviated away by further dipole magnets (B 5 + B 6) to a point 72 mm above the K_L beam at an upward angle of 3.6 mrad. Here they impinge on the K_S target, which has dimensions similar to the K_L target and is mounted in vacuum.

2.9 The K_S beam:

The layout of the K_S beam is shown schematically in Figure 8. The vertical displacement of the target with respect to the K_L beam is chosen to ensure that the two beams are separated by a sufficient lateral thickness of tungsten-alloy (~40 mm) to shield the K_L beam aperture against secondary particles emitted at forward angles (<~20 mrad.) from the target.

The K_S target and the following collimator apertures are aligned along an axis pointing downwards at 0.6 mrad., so as to intersect the (horizontal) K_L beam axis near the centre of the detectors, at a longitudinal distance from the K_S target of 120 m, as shown in Figure 9. This alignment is achieved by adjusting the transverse position of the target and steering the proton beam onto it, observing the centre of the neutral beam at the MONITOR STATION ~14 m downstream of the cross-over point. There the K_S axis should coincide horizontally with that of the K_L and be ~8.4 mm vertically below it.

SCAN TAGGING MONITOR COUNTERS vs TRIM-5 OF P42

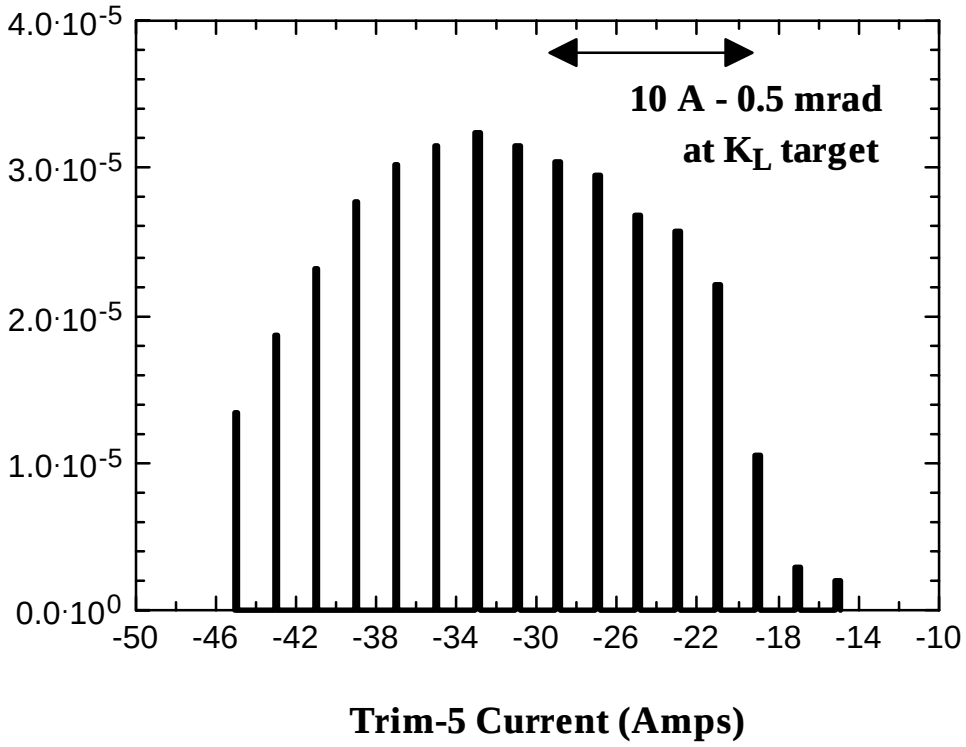

Fig. 6

Figure 6: Variation of proton transmission onto the scintillation counters at the TAGGING STATION (relative to proton flux incident on the K_L target: BSI), as a function of the current in Trim 5.

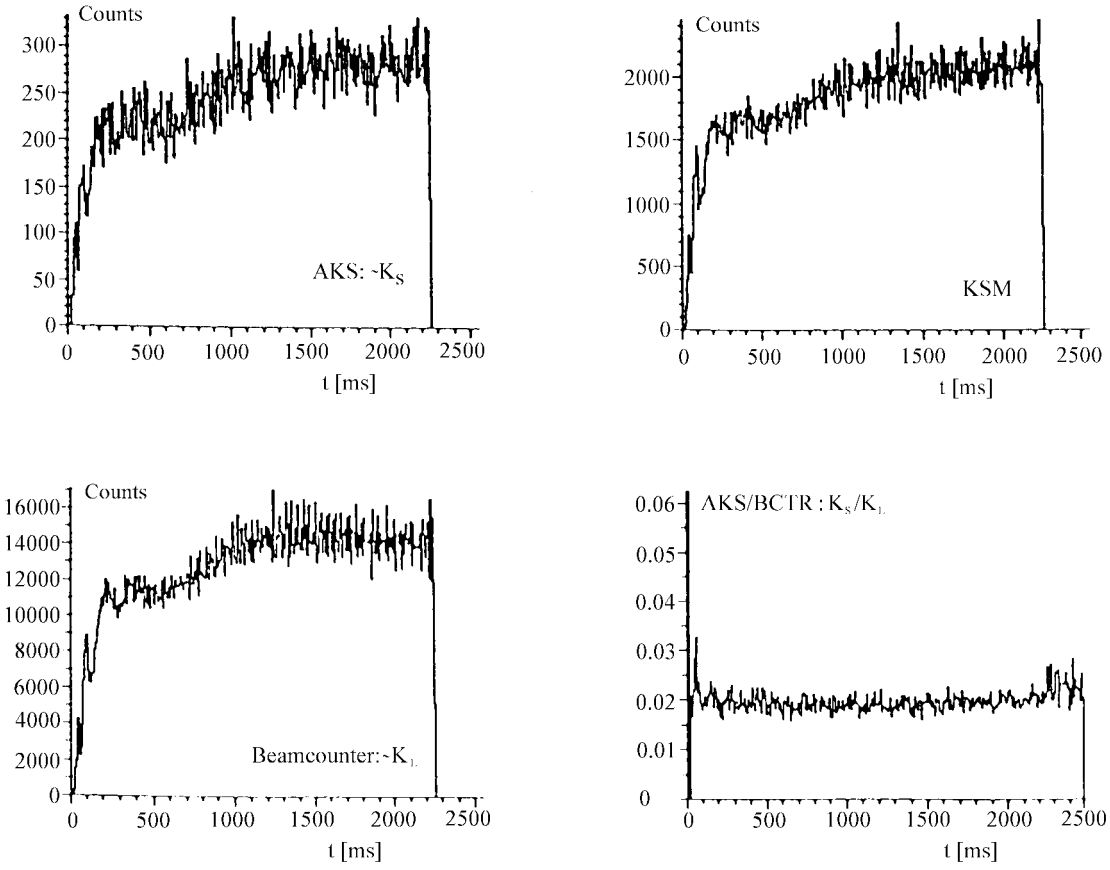

Figure 7: Displays of the time-variation of counting rates proportional to the K_S beam (AKS, KSM), to the K_L beam (BCTR) and of their ratio: K_S/K_L (AKS/BCTR) - over a SPS pulse (2380 ms).

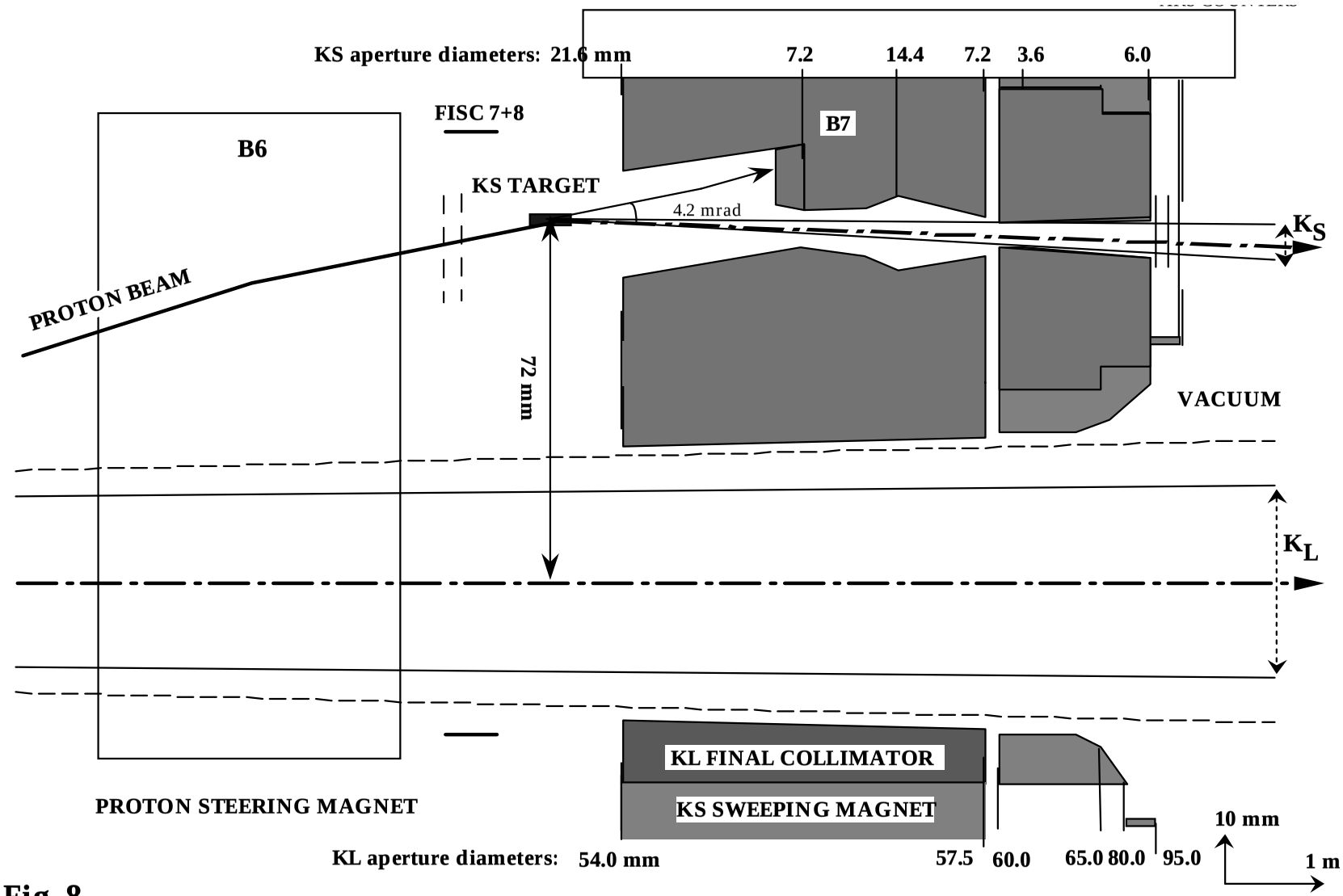

Fig. 8

Figure 8: Detailed layout of the K_S target station and beam, (vertical section).

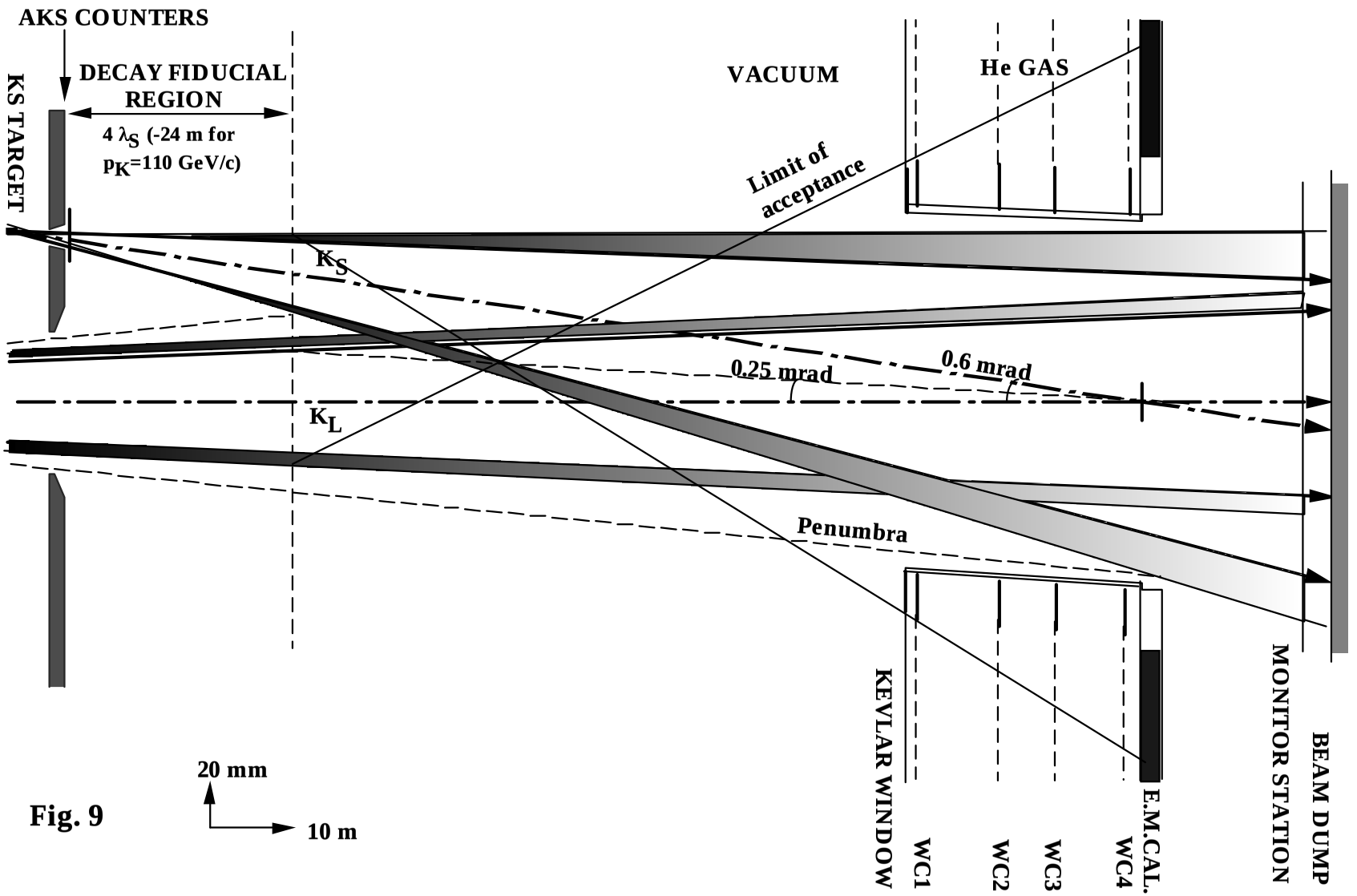

Fig. 9

Figure 9: Schematic layout of the K_L and K_S decay fiducial region and the passage of the beam through the centre of the detectors, (vertical section).

The resulting production angle of 4.2 mrad. for the K_S beam renders the ratio of K_S to K_L decays in the fiducial region (defined in units of λ_S) approximately equal at the two ends of the momentum range used, (p_K=70 and 170 GeV/c, see Section 1).

The K_S target is followed by a 7.5 T.m, vertical sweeping magnet (B 7), the gap of which is filled with tungsten-alloy inserts containing the passages for the two beams, (see Fig. 8). The passage for the K_S beam is shaped to absorb the remaining protons and charged secondary particles from the target, which follow curved trajectories in the field. The magnet is followed by a steel collimator block, which again contains precisely-bored passages for the two neutral beams, the one for the K_S being filled with inserts, graduated from a beam-defining aperture of 3.6 mm diameter at 4.8 m from the target to a final diameter of 6.0 mm at the exit, 6.0 m after the target. At this point, both K_L and K_S beams emerge into the common decay volume, pointing towards the detectors. For a given beam acceptance, the useful flux of K_S leaving the collimator relative to neutron-induced background from the edges of its defining aperture is maximised by the choice of the distance of that aperture from the target to be close to 1 λ_S.

2.10 Vacuum system:

Downstream of the last collimator (and the AKS counters, shown in Figs. 8 and 9), the vacuum chamber containing the two beams opens up into a cylindrical tank of total length 89 m and inner diameter 1.92 m increasing to 2.40 m, shown schematically in Figure 10. The enclosed volume serves to let the kaon decay products diverge unimpeded from the fiducial region of the respective beams towards the detector. The volume is evacuated in stages, by a set of trochoid, Roots and diffusion pumps, to a residual pressure $<10^{-4}$ mbar.

At its downstream end, the tank is closed off by a thin 'window' to separate the vacuum from the following volume, which is filled with helium gas, housing the drift chambers of the 'magnetic spectrometer', (shown in Fig. 10). The window is made of a 3-layer composite of epoxy-impregnated Kevlar tissue[2], draped and cured in a mould of spherical shape and 1.3 m radius of curvature. It is glued at its centre to an aluminium ring of outer diameter 184 mm and at its circumference to a steel flange of inner diameter 2.30 m. Over the area between these two flanges, the mean thickness of the window has been measured to be 0.9 mm, corresponding to $\sim 3.1 \cdot 10^{-3}$ of a radiation length, and the total leak rate for helium gas was found to be <1 mbar.l./s.

The window is mounted with its convex side facing into the vacuum tank, with the ring at its centre making a sliding seal onto the beginning of a tube of inner diameter 152 mm. This tube provides a passage in vacuum for the two convergent beams through the central apertures of all the succeeding detectors. The window and the following drift chambers, together with the tube, are centred along a line, which is inclined at a small downward angle (0.25 mrad.), close to the bisector between the K_L- and K_S-beam axes, (Fig. 9).

The beam tube was initially made of stainless steel throughout its length. The sections upstream of and in between the drift chambers were subsequently replaced by a tube of carbon-fibre composite with 1.2 mm wall-thickness, reinforced by ribs at 0.25 m intervals, and glued to aluminium end-flanges[3]. This tube is designed to reduce appreciably the probability for photons and electrons stemming from K_L decays to initiate high-multiplicity showers, which illuminate the drift chambers.

---

[2] The window used was manufactured (following a prototype, tested to destruction at an over-pressure >3 bar) by Elicotteri meridionali S.p.A., Anagni (I), using KEVLAR Style 285 pre-impregnated tissue.

[3] The tube was wound from HM-quality carbon fibres soaked with epoxy resin by Cowex AG., Faserverbundwerkstoffe, Pratteln (CH).

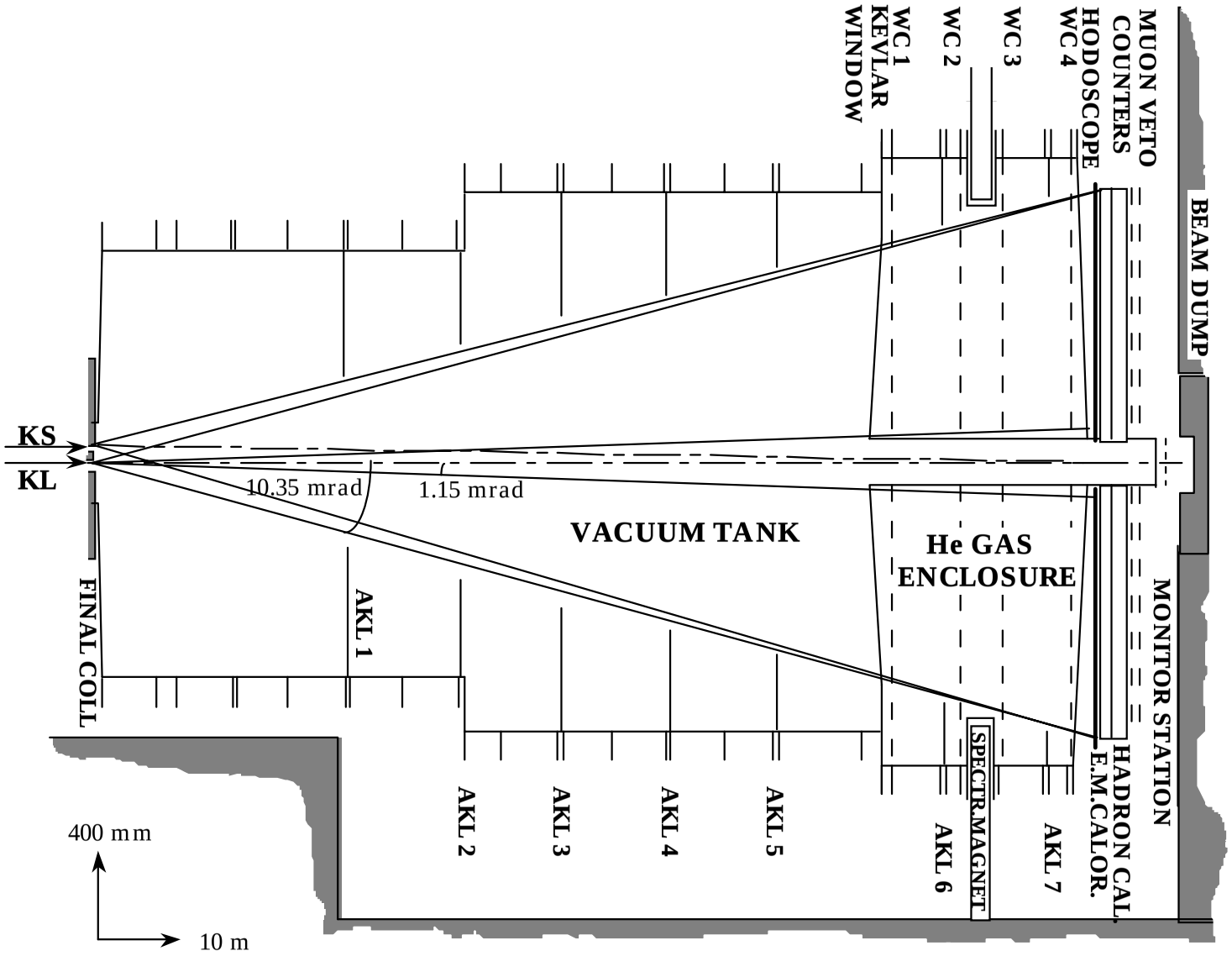

Fig. 10 Figure 10: Schematic layout of the decay vacuum tank and helium gas enclosure of the magnetic spectrometer, showing the Kevlar window and beam tube, (vertical section).

3. Beam observation and rates

3.1 Beam monitoring:

The primary proton beam line to the K_L target is equipped with secondary emission monitors (SEM), consisting of foils of aluminium housed in vacuum, on which the charge induced by the beam can be measured (in the flux range: 10^{10}-10^{13} protons per pulse). The total flux of protons is measured on single foils (BSI) covering the whole beam. One such foil, in front of the K_L target, is made of aluminium; another, made of titanium, installed further upstream where the beam is larger, has the advantage that its response is more stable in time. The signals from these foils have been calibrated against an absolute measurement of the γ-emission of the isotope ^{24}Na, produced in a foil of pure Al, temporarily exposed to the beam, [7].

In other types of SEM the foil is split in half (BSP) or forms a filament (BBS) that can be scanned across the beam, respectively allowing the asymmetry in position or the profile of the beam to be measured upstream of the target. An example of the horizontal and vertical profiles obtained at the final focus is shown in Figure 11.

Downstream of the bent crystal, the flux of the transmitted proton beam is monitored on a pair of scintillation counters at the TAGGING STATION, (Fig. 3). The steering of the beam through the K_L collimators and its focusing onto the K_S target are observed using filament scintillation counters (FISC), which can be scanned across the beam in vacuum. Profiles obtained just in front of the K_S target using FISC 7 + 8, (Fig. 8), are shown in Figure 12.

At the end of the neutral beam line (254 m from the K_L target), the vacuum tube is closed off by a 0.1 mm thick Mylar window just in front of the MONITOR STATION, (Fig. 2). In order along the beam, this comprises the following series of monitors, which are used to adjust the K_L and K_S beams separately and to record essentially the K_L component in the simultaneous beams:

i) A pair (horizontal and vertical) of special FISC counters (FISC 9 + 10), in which the scintillator filaments, each of [4 · 4] mm^2 cross-section, have copper strips of similar dimensions attached to their leading edges. By scanning them across the beam in turn, these counters provide profiles of the respective neutral beams by conversion, mainly of the photons, in the copper. Typical profiles of the K_L and of the K_S beams are shown in Figure 13.

ii) A multi-wire-proportional chamber (MWPC) with horizontal and vertical wire planes, equipped with analogue read-out and preceded by a (retractable), 5 mm thick, aluminium converter. Since, (in contrast to the FISC), the converter covers the whole beam, the profiles obtained show tails, due to illumination from locally-produced, large-angle Bremsstrahlung. Nevertheless, the MWPC serves to provide quick checks of the K_L beam and to locate the beam axes in the alignment of the K_L and the K_S beams, (Sections 2.4 and 2.9).

iii) A scintillation counter (TRIG), 200 mm in diameter, covering the whole beam aperture. In conjunction with the MWPC, it is used (without the converter) to tune the transmitted proton beam, which is initially directed on axis, or (with converter in front), to check either the K_S or the K_L neutral beam.

iv) A beam monitor (BCTR), used to record the flux of the neutral beams. It differs from the TRIG counter in that the beam profile is sampled in horizontal and vertical projections using scintillating fibre bundles, spaced 7.8 mm. apart. Each bundle is composed of 18 square fibres of 0.5 mm width, stacked in the beam direction. Groups of 3 bundles are read out by a common photomultiplier. The signals are discriminated and counted in a latching scaler with a sampling time of 7.5 ms. This is also done for other counters (including the tagging counter), used to monitor the beam rates, (Section 2.7), and allows modulations up to 60 Hz. to be recorded together with the physics data for each SPS pulse. Effective spill lengths of typically 1.5 - 1.8 s. are found (for 2.38 s. spill duration).

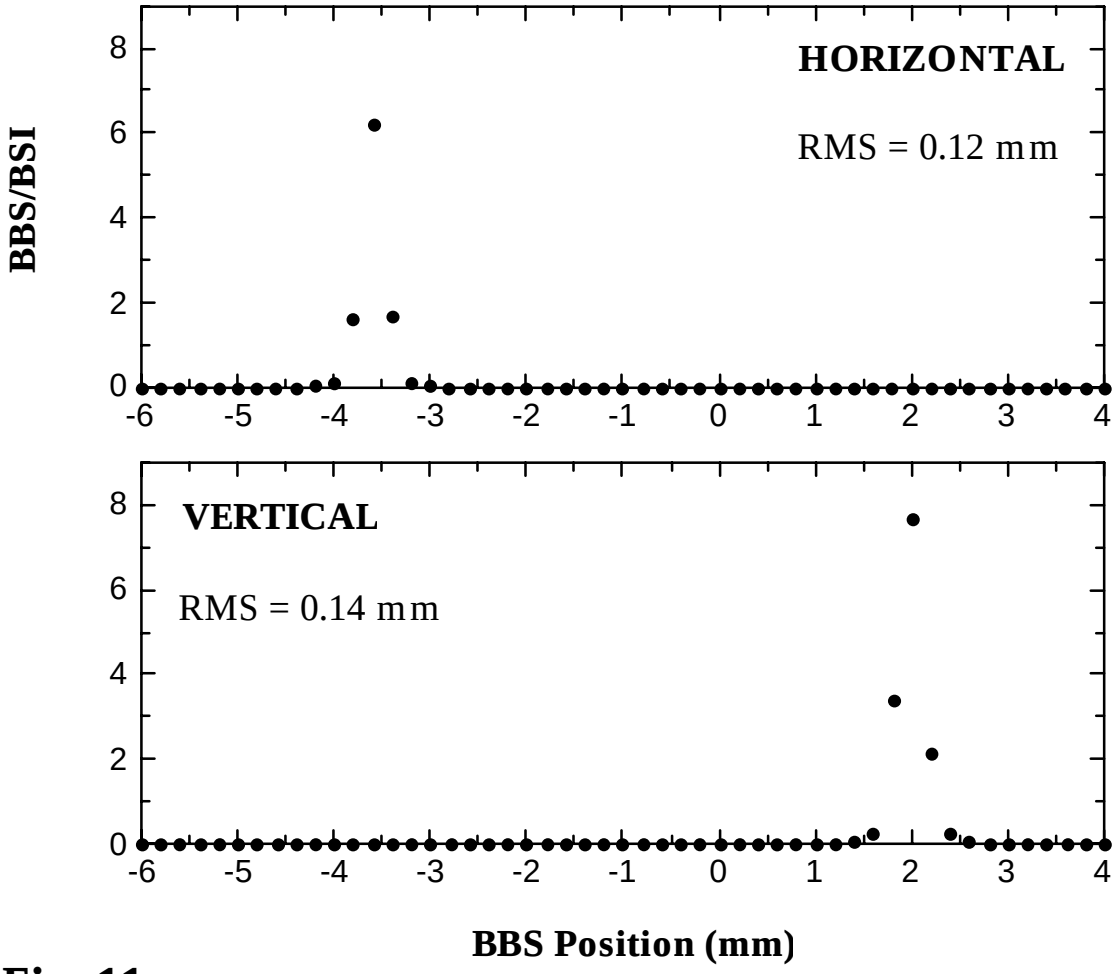

Fig. 11

Figure 11:Horizontal and vertical profiles of the primary proton beam at the focus onto the K_L target, measured with SEM filament scanners: BBS, (normalised to total flux recorded on BSI).

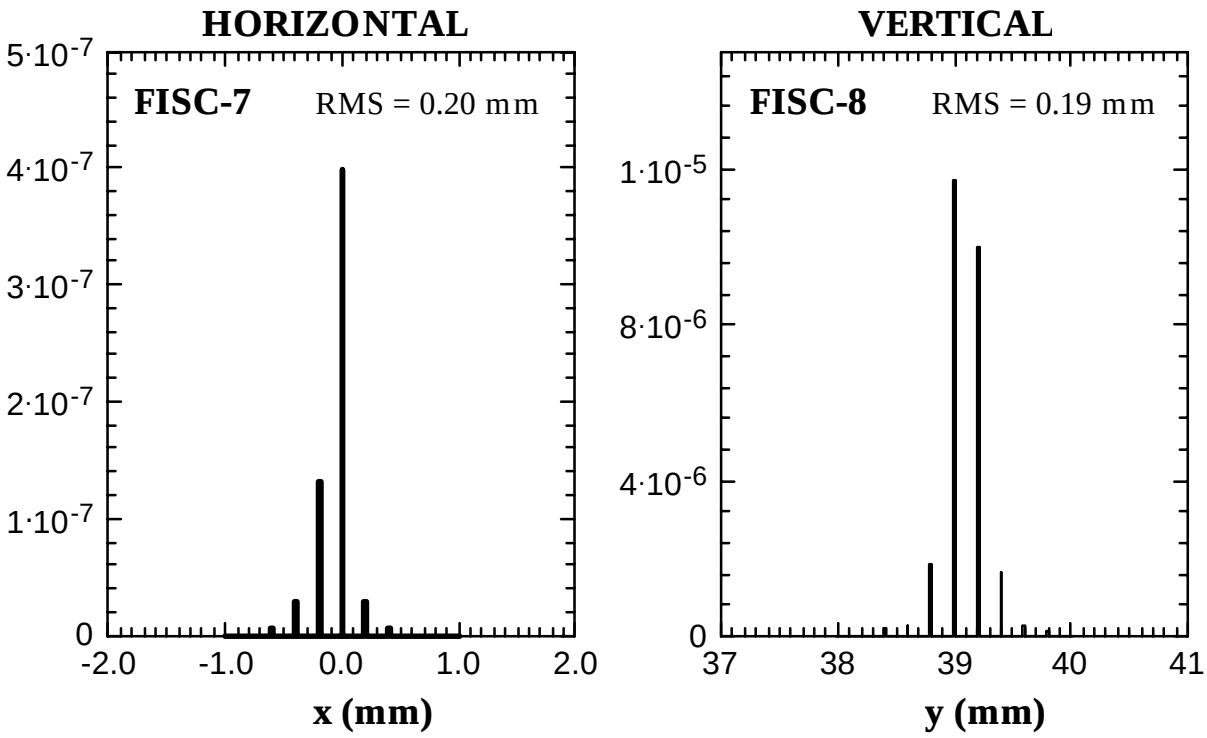

Fig. 12

Figure 12:Horizontal and vertical profiles of the proton beam incident onto the K_S target, measured with (0.2 mm wide) filament scintillation counters: FISC 7 + 8, (normalised to flux on K_L target: BSI).

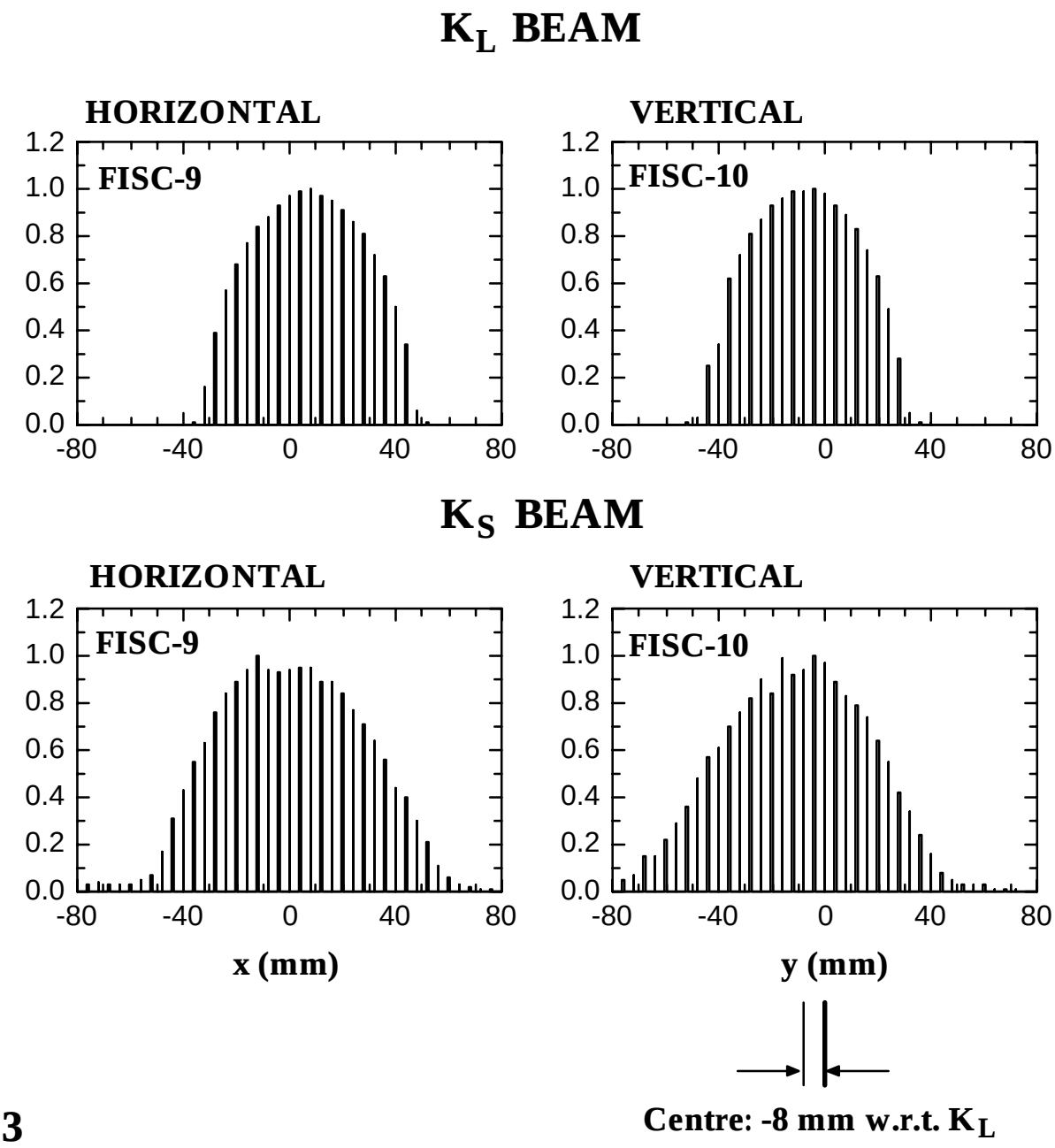

Fig. 13

Figure 13: Horizontal and vertical profiles of the K_L and K_S neutral beams, measured separately, counting charged particles from conversion in the (4 mm wide) Cu strips attached to FISC 9 + 10 of the MONITOR STATION. (The upstream converter normally preceding the AKS counters was removed, so as not to degrade the profiles of the K_S beam).

3.2 Choice of beam modes:

An important feature of the dump/collimators (TAX), installed at the beginning of the primary proton beam (Section 2.2) and downstream of the K_L target (Section 2.3), is that they can be displaced vertically and so present a choice of apertures to the beams that pass through them. Those in the primary beam allow the flux of protons to the K_L target to be varied in six discrete steps, ranging from $<10^{11}$ up to the nominal $1.5 \cdot 10^{12}$ per pulse, in addition to having a position where the beam can be dumped.

The second dump/collimator following the K_L target, (TAX 18, Fig. 3), is fitted with tungsten-alloy inserts having apertures matched to the envelopes of the wanted beams of K_L (Section 2.3) and of protons for K_S (Section 2.8), respectively. It generally remains in a fixed position during operation of the neutral kaon beams. The first, (TAX 17), is fitted with two sets of inserts, which have similar, larger apertures, at the vertical separation (72 mm) corresponding to the two beams and a set of 'blind' inserts at a similar distance below the lower aperture. By suitable vertical positioning of TAX 17, either the K_L alone or the protons for K_S alone, or both, simultaneous K_L+K_S beams, can be transmitted. In the K_L-only mode, the K_S-proton beam strikes and is absorbed in the blind inserts of TAX 17. In the K_S -only mode, the unwanted K_L beam is similarly absorbed in the material (0.4 m Fe + 1.2 m Cu) of TAX 17, leaving $<\sim 10^{-3}$ of the K_L flux to be transmitted.

The modes, in which only one of the two beams is present at a time, are used in setting up the beam and the detectors. They are also of interest in analysing the contributions to the total K_L+K_S counting rates recorded by the detectors according to three distinct sources. These can be identified from differences in counting rates among the three modes, [K_L], [K_S] and [K_L+K_S]:

Thus,

Contribution from the K_L beam downstream of TAX 17: K_L=[K_L+K_S]-[K_S];

Contribution from the K_S beam

- including K_S proton transport downstream of TAX 17: K_S=[K_L+K_S]-[K_L];

Contribution to background from the K_L target station

- including proton dump in TAX 17: *Background* =[K_L+K_S]-K_L-K_S=[K_L]+[K_S]-[K_L+K_S].

3.3 Counting rates:

Typical counting rates, recorded by the principal detectors in each of the three beam modes: [K_L], [K_S] , [K_L+K_S], are indicated in Table II. The rates are those measured in 1997 with the beam tube linking the drift chambers still made of stainless steel, (Section 2.10). These rates are also analysed according to their respective sources: K_L, K_S and *Background*, as defined above (Section 3.2).

4. Calibration beams

Alternatively to the neutral kaons, it is possible to provide beams of muons, negatively-charged pions and kaons, or electrons at different momenta to set up and to calibrate the detectors.

4.1 Muons:

Muons are obtained by stopping both beams, K_L and protons for K_S, in the dump/collimators following the K_L target (TAX 17 + 18, Fig. 3) and switching off the magnetic 'scraper' and subsequent sweeping magnets, (Section 2.5). This provides a rather uniform illumination of the detectors by the muons from decay of pions produced in the K_L target and proton dump. At nominal primary proton flux, a typical intensity of $\sim 3 \cdot 10^5$ μ/m^2 per SPS pulse is observed.

4.2 Negatively-charged pions and kaons:

By suitable choice of the strengths of the deflecting magnets: B 1, B 2, B 3 and positions of TAX 17 + 18 (Fig. 3), it is possible to direct a beam of negatively-charged, secondary particles from the K_L target onto the K_L beam axis, (dashed trajectory in Fig. 3). If the subsequent dipole and quadrupole magnets (B 5, B 6, B 7, Q 1 + 2) are switched off, this beam follows a path, which is defined by the collimators to be similar to that of the K_L beam. It has a broad momentum spectrum, ranging from ~0.7 p_π to ~1.6 p_π about the chosen central momentum, p_π. For p_π = 75 GeV/c and $1.5 \cdot 10^{11}$ primary protons per pulse incident on the K_L target, a beam of total flux $\sim 1 \cdot 10^7$ per pulse is obtained, composed mainly of π^- and K^- in a ratio of ~15 : 1. The beam is made to impinge on a thin polyethylene target, which can be inserted into the vacuum chamber at the beginning of the K_L fiducial region. This serves as a copious source of charged particles and of π^0 and η^0 decaying into photons, which illuminate the detectors and allow an accurate calibration of the reconstructed position of the source to be made.

4.3 Electrons:

Electrons are produced by photons issuing from the target, T4, traversed by the primary proton beam 838 m upstream of the K_L target, (Section 2.2). In this mode, charged particles from the target are swept into the following dump/collimators, leaving mainly photons to impinge on a lead converter at the beginning of the beam line. The subsequent beam transport and collimators on the line leading to the K_L target are used to define a beam of electrons with >~99 % purity and intrinsic momentum spread ±0.1 % of the central momentum, p_e (chosen from 15 to 100 GeV/c). The flux can be varied in the range: 10^2-10^4 electrons per pulse. This beam is directed onto the K_L axis, passing through the K_L target station with the target retracted and through the subsequent collimators. It is focused at the longitudinal position of the K_S target and then diverges towards the detectors. Using the last two dipole magnets (B 6 + B 7 in Fig. 8), it can be deflected out of the downstream beam tube to illuminate an area of ~60 cm^2 around any point on a vertical strip of the electromagnetic calorimeter. Alternatively, it can be deflected onto the trajectory of the K_S beam, so as to pass through the AKS counters, located at the exit of the K_S collimator, (Fig. 8).

Acknowledgements

We wish to acknowledge the contributions and support of our colleagues in the NA48 collaboration, within the framework of which the simultaneous K^0 beams have been conceived and designed, and together with whom this report is intended to be published. Our special thanks are due to E. Uggerhøj (Aarhus University, Denmark), who provided the Si crystals and who, together with our colleagues K. Elsener, S.P. Møller and U. Mikkelsen of the Aarhus-CERN-Strasburg 'Bent Crystal Collaboration' furthered our understanding of particle channeling in crystals. We are indebted to members of many groups in SL- and other Divisions in CERN, who participated in the construction, installation and control of the beams and their components. We explicitly wish to mention: M. Clément, G. Dubail, C. Ferrari, B. Tomat, P. Pierre, R. Allegrini, B. Chauchaix, W. Boult, A. Bonifas (SL/EA); K.D. Lohmann, C. Beugnet, G.P. Ferri, G. Ferioli (SL/BI); S. Peraire, M. Ross, G. Del Torre, A. Hilaire (SL/BT); K. Cornelis, G. Arduini, G. Roy (SL/OP); A. Simon (EST/MF); M. Hayotte, M. Chambardon (EST/SU); M. Mathieu, R. Rey (EST/ESM); G. Stevenson, G. Bertuol, J.C. Gaborit (TIS/RP).

References

[1] G.D. Barr et al., CERN, Edinburgh, Mainz, Perugia, Pisa, Saclay, Siegen, Torino, Vienna Collaboration, "Proposal for a Precision Measurement of ε'/ε in CP-violating $K^0 \to 2\pi$ Decays", CERN/SPSC/90-22, SPSC/P253, 20 July 1990.

[2] G. Brianti, N. Doble, "The SPS North Area High Intensity Facility: NAHIF", CERN/SPS/EA 77-2, CERN/SPSC/77-72, SPSC/T-18, 16 August 1977.

[3] Ch. Iselin, "HALO: A Computer Program to calculate Muon Halo", CERN 74-17, 29 August 1974.

[4] S.P. Møller et al., Nucl. Instr. and Meth. B 84 (1994) 434.

[5] A. Baurichter et al., Nucl. Instr. and Meth.. B 119 (1996) 172.

[6] N. Doble, L. Gatignon, P. Grafström, Nucl. Instr. and Meth. B 119 (1996) 181.

[7] K. Bernier et al., "Calibration of Secondary Emission Monitors of Absolute Proton Beam Intensity in the CERN SPS North Area", CERN 97-07, 3 July 1997.